



Source impact and contribution analysis of ambient ozone using multi-modeling approaches over the Pearl River Delta region, China[☆]

Tingting Fang^a, Yun Zhu^{a,b,*}, Shuxiao Wang^c, Jia Xing^c, Bin Zhao^c, Shaojia Fan^b, Minhui Li^d, Wenwei Yang^a, Ying Chen^a, Ruolin Huang^a

^a Guangdong Provincial Key Laboratory of Atmospheric Environment and Pollution Control, College of Environment and Energy, South China University of Technology, Guangzhou Higher Education Mega Center, Guangzhou, 510006, China

^b Southern Marine Science and Engineering Guangdong Laboratory (Zhuhai), Sun Yat-Sen University, Zhuhai, 519000, China

^c State Key Joint Laboratory of Environment Simulation and Pollution Control, School of Environment, Tsinghua University, Beijing, 100084, China

^d Guangdong Provincial Academy of Environmental Science, Guangzhou, 510006, China

ARTICLE INFO

Keywords:

O₃
Air quality model
Response surface modeling
Source impact
Source contribution

ABSTRACT

Quantification of source impacts and contributions is a key element for the design of effective air pollution control policies. In this study, O₃ source impacts and contributions were comprehensively assessed over the Pearl River Delta (PRD) region of China using brute-force method (BFM), response surface modeling with BFM (RSM-BFM) and differential method (RSM-DM) respectively, high-order decoupled direct method (HDDM), and ozone source apportionment technology (OSAT). The multi-modeling comparison results indicated that under typical nonlinear atmospheric conditions during the O₃ formation, BFM, RSM-BFM, and HDDM seemed to be appropriate for assessing the impact of single source emissions; however, the results of HDDM could deviate from those of BFM when the emission reduction ratio was higher than 50 %. Under multi-source control scenarios, the results of source contribution analyses obtained from RSM-DM and OSAT were reasonably well, but the performance of OSAT was limited by its capability in representing the nonlinearity of O₃ response to emission reductions of its precursors, particularly NO_x. The results of this pilot study in the PRD showed that the RSM-DM appeared to replicate the nonlinearity of O₃ chemistry reasonably well (e.g., O₃ disbenefits due to local NO_x emission reductions in Guangzhou city). Based on the source contribution results, on-road mobile (including both NO_x and VOC emissions) and industrial process (mainly VOC emissions) sources were identified as two major contribution sectors by both RSM-DM and OSAT, contributing an average of 31.5 % and 11.4 % (estimated by RSM-DM) and 29.2 % and 13.0 % (estimated by OSAT) respectively to O₃ formation in 9 cities of the PRD. Therefore, the reinforced emission reductions on NO_x and VOC from on-road mobile and industrial process sources in the central cities (i.e., Guangzhou, Foshan, Dongguan, Shenzhen, and Zhongshan) were suggested to effectively mitigate the ambient O₃ levels in the PRD.

1. Introduction

Tropospheric ozone (O₃) is an important air pollutant that exerts significant effects on human health and ecosystems (Feng et al., 2015; Grulke and Heath, 2020; Li et al., 2019a; Liu et al., 2018; U.S. EPA, 2020; Wu et al., 2019). After a period of rapid economic growth and urbanization, O₃ pollution has emerged as a serious environmental issue over the Pearl River Delta (PRD) region of China (Gao et al., 2020; Gong et al., 2018; Li et al., 2019b; Liu et al., 2018; Liu et al., 2020; Shen et al.,

2019). The yearly 90th percentile of the daily maximum 8-h average (MDA8) O₃ concentrations in the PRD have continuously exceeded 160 μg m⁻³ (the China grade II national air quality standard, ~80 ppbv) from 2017 to 2019, even as the concentrations of fine particulate matters (PM_{2.5}) have evidently decreased (DEPGP, 2020). Forming effective emission control strategies for reducing O₃ concentrations is usually challenging due to the complexity of the photochemical reactions involving nitrogen oxides (NO_x) and volatile organic compounds (VOCs) that drive the O₃ formation (Liu et al., 2019; Wang et al., 2019), as well

[☆] This paper has been recommended for acceptance by Pavlos Kassomenos.

* Corresponding author. Guangdong Provincial Key Laboratory of Atmospheric Environment and Pollution Control, College of Environment and Energy, South China University of Technology, Guangzhou Higher Education Mega Center, Guangzhou, 510006, China.

E-mail address: zhuyun@scut.edu.cn (Y. Zhu).

<https://doi.org/10.1016/j.envpol.2021.117860>

Received 10 June 2021; Received in revised form 7 July 2021; Accepted 26 July 2021

Available online 27 July 2021

0269-7491/© 2021 Elsevier Ltd. All rights reserved.

as the diversity of emission sources that contribute to O₃ (Gao et al., 2020; Li et al., 2012). Hence, identifying the influence of major emission sources on O₃ has become a key quest for policymakers and scientists (Hallquist et al., 2016; Thunis et al., 2019).

The primary modeling techniques within the chemical transport models (CTMs) used for air quality management can be classified into source impact and source contribution methods (Baker and Kelly, 2014; Clappier et al., 2017; Cohan et al., 2005; Dolwick et al., 2015; Thunis et al., 2019). Source impact methods estimate the response of O₃ concentrations to a reduction of individual source emissions to calculate the single source impact (Luecken et al., 2018; Wang et al., 2011b), while source contribution (or apportionment) methods attribute a fraction of the O₃ concentrations to precursor emissions from a given source to compute the single source contribution (Li et al., 2016; Moghani et al., 2018). In the case of linear relationships between pollutant concentrations and precursor emissions, source impact and contribution methods can be used interchangeably to estimate the impacts of individual emission source reductions on O₃ or the contributions of various emission sources to O₃. However, under typical nonlinear atmospheric conditions where the interactions among multiple emissions sources are non-negligible, source impact methods are more suitable for air quality planning applications to assess the impact of a single source abatement strategy, while source contribution methods are more applicable for analyzing the apportionments of O₃ concentrations attributed to various source emissions (Clappier et al., 2017; Dunker et al., 2002; Kwok et al., 2015; Thunis et al., 2019).

The brute-force method (BFM) and the high-order decoupled direct method (HDDM) are source impact methods that have been broadly applied in previous studies (Burr and Zhang, 2011a; Collet et al., 2017; Couzo et al., 2016; Itahashi et al., 2020; Kim et al., 2017; Luecken et al., 2018; Zhang et al., 2012). BFM involves conducting the baseline and emission-perturbed simulations and estimating the source impact from the difference in concentrations between these two CTM simulations (Burr and Zhang, 2011a). BFM can exactly characterize the impact of a specific emission source reduction scenario (Chen et al., 2019). However, it is computationally expensive for BFM to measure the impacts of a large number of emission control scenarios, because BFM needs a separate simulation for each perturbation (Cohan et al., 2005; Yang et al., 1997). HDDM numerically calculates the O₃ sensitivities to changes in precursor emissions by solving the derivatives of the partial differential equations governing the CTM (Dunker, 1984; Hakami et al., 2003, 2004; Itahashi et al., 2020; Itahashi et al., 2013; Luecken et al., 2018), and the sensitivity coefficients estimated by the HDDM have been proven to reliably represent the impacts of emission perturbations on O₃ when the emission reduction ratio was less than about 50 % (Cohan et al., 2005; Couzo et al., 2016; Itahashi et al., 2015). However, the accuracy of HDDM degrades compared with the BFM for large emission reductions (Cohan et al., 2005; Huang et al., 2017), and HDDM also becomes relatively inefficient for cases where the number of emission control factors is greater than 3 (Zhao et al., 2015).

Source contribution modeling techniques include ozone source apportionment technology (OSAT) (Yarwood et al., 1996) and integrated source apportionment method (ISAM) (Byun and Schere, 2006; Foley et al., 2010), and both of them have been widely used for O₃ source contribution analysis due to their simple formulations and high efficiencies (Collet et al., 2018; Ge et al., 2021; Han et al., 2018; Kwok et al., 2015; Li et al., 2016; Li et al., 2012; Lu et al., 2016; Shu et al., 2020; Wang et al., 2009; Yang et al., 2021; Zhang et al., 2017). OSAT and ISAM are capable of apportioning O₃ source contributions from multiregional and multisectoral emissions simultaneously based on a single model run, in which the sum of individual contributions is equivalent to the total O₃ concentrations (Chatani et al., 2020; Moghani et al., 2018; Thunis et al., 2019). Source apportionment techniques were not developed to represent the nonlinear response of O₃ to emission changes (e.g. O₃ disbenefits associated with NO_x reductions in NO_x-saturated areas (Chatani et al., 2020; Itahashi et al., 2015)), but under the

assumption of linear response, source apportionment techniques may be also used to estimate the impact of emission changes on O₃ response in some cases (Clappier et al., 2017; Kwok et al., 2015; Thunis et al., 2019).

Response surface models (RSMs) are another approach that has recently been applied in estimating source impacts and contributions. RSMs are developed by statistically fitting the results of multiple CTM simulations with the emission changes relative to the base case, and once established, RSMs can predict the O₃ response to emission changes in near real-time (Xing et al., 2011). The RSM technique was initially developed by USEPA, 2006 and then continuously improved by our research team over the past several years (Jin et al., 2020; Wang et al., 2011a; Xing et al., 2019; Xing et al., 2018; Xing et al., 2020a; Xing et al., 2011; Xing et al., 2017; Xing et al., 2020b; You et al., 2017; Zhao et al., 2015; Zhao et al., 2017; Zhu et al., 2015). The traditional RSM with BFM (RSM-BFM) has been used for assessing source impacts and contributions, but RSM-BFM has the limitation in effectively quantifying the nonlinear contribution of precursor emissions from multiple source regions (Fang et al., 2020; Pan et al., 2020), hence a new differential method within the RSM (RSM-DM), which divides the emission perturbations into plenty of tiny ranges and regards the sum of the O₃ response in each range as the source contribution, was proposed by Fang et al. (2020) to address this limitation.

Although the aforementioned modeling techniques (e.g., BFM, RSM-BFM, HDDM, RSM-DM, and OSAT) have previously been applied for both source impact and contribution analysis, the underlying algorithms of individual techniques are fundamentally different, as they were developed to address different questions (Clappier et al., 2017; Thunis et al., 2019). Comparative analysis of different methods is needed to understand the O₃ source impacts and contributions more comprehensively and appropriately, and clarify the applicability of each approach for developing effective O₃ control strategies; but such a comparative evaluation was only conducted in limited case studies of the United States, Europe and East Asia (Burr and Zhang, 2011b; Chatani et al., 2020; Cohan et al., 2005; Dolwick et al., 2015; Dunker et al., 2002; Itahashi et al., 2015; Koo et al., 2009; Kwok et al., 2015). In this study, we conduct a comparative analysis of O₃ source impacts and contributions over the PRD region of China using BFM, RSM-BFM, HDDM, RSM-DM, and OSAT. The similarities and discrepancies among these techniques are analyzed, and the applicability of each method in supporting the policy-making is also discussed together with the suggestions given for O₃ mitigation in the PRD based on this study.

2. Methodology

This study follows the scheme shown in Fig. 1 to conduct O₃ source impact and contribution analysis over the PRD region. First, the emission sources of O₃ for which impacts and contributions were estimated were selected; second, the modeling domain and configuration were determined to drive the Weather Research and Forecasting-Community Multiscale Air Quality Model (WRF-CMAQ) and WRF-Comprehensive Air Quality Model with Extensions (WRF-CAMx) simulations over the PRD, and the RSM was constructed subsequently on the basis of the CMAQ simulations; then, multiple numerical and chemical techniques, including the RSM with BFM (RSM-BFM) and a newly differential method (RSM-DM) respectively, BFM and HDDM based on the CMAQ, and the built-in OSAT in the CAMx, were exploited to comprehensively evaluate the multiregional O₃ source impacts and contributions in the case study of the PRD; lastly, for specifying the contribution from each sector, the multiregional source contributions were further separated into that from different sectors using RSM-DM and OSAT.

2.1. Modeling domain and configuration

The CMAQ in version 5.2 (<http://www.epa.gov/cmaq>) and CAMx in version 7.0 (<http://www.camx.com/>) were utilized to perform the O₃ simulations, and the meteorological inputs derived from the WRF in

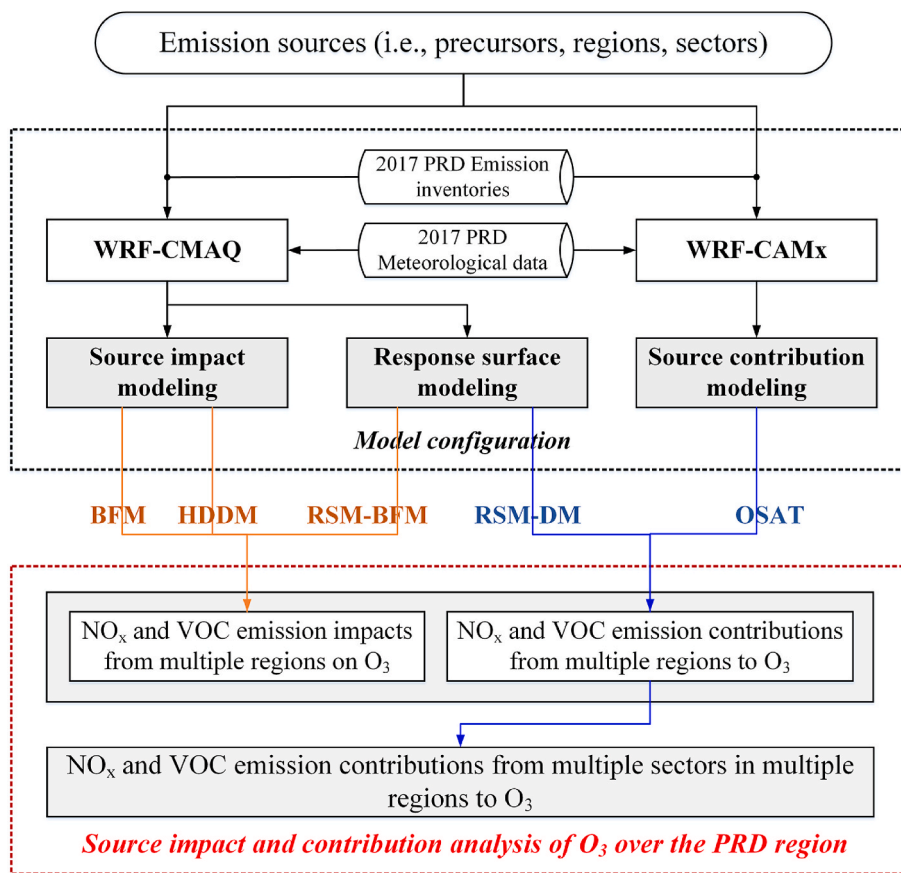


Fig. 1. The flow scheme for source impact and contribution analysis of O₃ using multiple modeling approaches over the PRD region.

version 3.9.1 (<http://www2.mmm.ucar.edu/wrf/>) were provided for both CMAQ and CAMx. The simulation domain of both two models was three nested with 27 km, 9 km, and 3 km horizontal resolutions, while the third domain covered the entire PRD Region, which was similar to that in our previous research (Fang et al., 2020). The source regions in

the D3 domain were divided into Guangzhou (GZ), Foshan (FS), Zhongshan and Zhuhai (ZS&ZH), Jiangmen (JM), Dongguan and Shenzhen (DG&SZ), and Zhaoqing and all the other areas (ZQ&OTH) in this study; the receptor regions included 9 cities in the PRD, and the air quality in each city was represented by the overall of the state-controlled

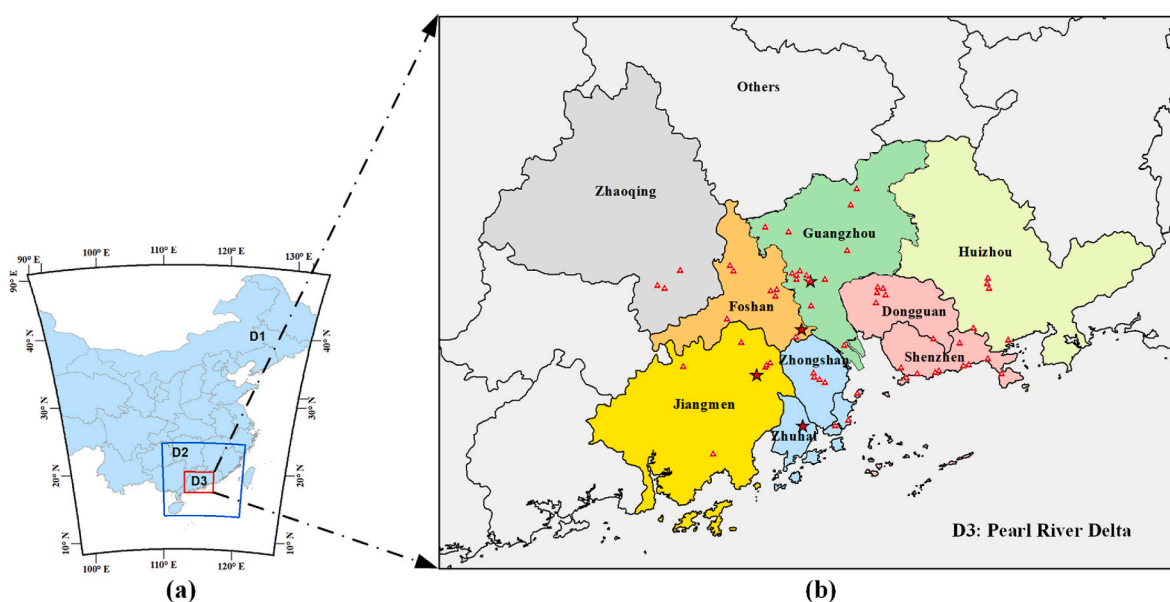


Fig. 2. (a) Three nested modeling domains with 27 km, 9 km, and 3 km horizontal resolutions, respectively, and (b) the Pearl River Delta (PRD) region in the D3 domain. Triangular points in the D3 domain represent the state monitoring sites in each city of the PRD; pentacle points represent the selected monitoring sites for evaluation of the model performance.

air-monitoring sites (Fig. 2). Both models generated the initial and boundary conditions based on the default configuration, and the simulations in the first and second domains were supplied to drive the boundary conditions for 9-km in the middle and 3-km inside respectively. Emission inventories of the first and second domains were offered by Tsinghua University (Wang et al., 2014; Zhao et al., 2018), and the inner 3-km domain utilized the recently developed 2017-based PRD regional emission inventory. To estimate O₃ source impacts and contributions in the PRD, the regional emission groups were separated into anthropogenic NO_x and VOC emissions from 7 source regions in the D3 domain respectively, while the sectoral emission groups were categorized by NO_x emissions from on-road mobile, non-road mobile, stationary combustion, and other all sources, and VOC emissions from on-road mobile, industrial process, solvent utilization and other sources (Table 1); the spatial distribution of each sectoral NO_x and VOC emissions was displayed in Fig. S1 and Fig. S2, respectively. The chemical mechanism used in both CMAQ and CAMx was the Carbon Bond version 6 (CB6) (Stockwell et al., 2020; Yarwood et al., 1997). The detailed parameter configurations of CMAQ and CAMx are shown in Table S1. It should be noted that the different parameter configurations and schemes of CMAQ and CAMx could inevitably cause some additional variabilities in the simulation results of the two models, but these variabilities will not have an obvious effect on our source impact and contribution analysis results, because the emissions and meteorology inputs and the used gas-phase chemistry mechanism were the same for CMAQ and CAMx in our study. The performance of CMAQ and CAMx for O₃ simulation and the correlation between the two models are detailed in Supporting Information (SI).

In 2017, the PRD suffered apparent O₃ pollution in the autumn season, especially in September, when the monthly maxima of the hourly averaged ozone in most sites of the Guangdong-Hong Kong-Macao Pearl River Delta Regional Air Quality Monitoring Network exceeded 200 µg m⁻³ (the China Grade II National Air Quality Standard, ~100 ppbv) (HKEPD, 2017). Accordingly, for evaluating O₃ source impacts and contributions in a typical ozone-polluted month, September in 2017 was selected for conducting CMAQ and CAMx simulations, and a spin-up time of 5 days was determined to eliminate the effect of initial conditions in both models.

2.2. Multiple modeling approaches

For multiple methods utilized in this study, in the field of source impact analysis, BFM, RSM-BFM, and HDDM can evaluate the impact of

Table 1
Emission groups for which source impacts and contributions were estimated.

Emission Groups	Precursors	Sources	Estimations
Region	NO _x , VOC	Guangzhou (GZ) Foshan (FS) Zhongshan and Zhuhai (ZS&ZH) Jiangmen (JM) Dongguan and Shenzhen (DG&SZ) Huizhou (HZ) Zhaoqing and all the other areas in the D3 domain (ZQ&OTH)	Source impacts and contributions
Sector	NO _x	On-road mobile Non-road mobile Stationary combustion Others (industrial process, and biomass burning)	Source contributions
	VOC	On-road mobile Industrial process Solvent utilization Others (storage & transportation, waste treatment, biomass burning, and non-road mobile)	

a given emission source on O₃ based on the difference in O₃ concentrations under the base and single source control scenarios, in which BFM follows the “zero-out” theory to directly regarding this difference as the single source impact; RSM-BFM follows the same principle as the BFM but uses more flexible polynomial functions to represent the atmospheric processes and calculate the source impact mathematically; HDDM builds a relationship between the O₃ response to emission changes in individual sources through some defined sensitivity coefficients mathematically approximated from the BFM’s calculations (detailed in Section 2.2.1). For source contribution analysis, RSM-DM and OSAT can quantify the source contribution to O₃ through mathematically and chemically attributing a fraction of the O₃ concentrations to specific source emissions, respectively, for which RSM-DM differentiates the emission changes into plenty subtle intervals and sums up the O₃ response in each interval as the source contribution (detailed in Section 2.2.3); OSAT tracks the O₃ formation at any time through a series of chemical tracers and allocates the contribution to the corresponding source subsequently (detailed in Section 2.2.2). The fundamental difference between the impact and contribution is that the “impact” usually contains the direct impact together with the indirect effects (denoted as the influence of the interactions among multiple emission sources under a nonlinear system), while the “contribution” separates the indirect effects and mixes them with the direct impact to represent the direct contribution of a specific source (Chatani et al., 2020; Clappier et al., 2017; Cohan et al., 2005; Thunis et al., 2019). Fig. 3 gives a simple illustration of the process of each method for calculating the impact and contribution of an example source, NO_x emissions from source region A, and the principle of each method is introduced in the following three sections.

2.2.1. Source impact modeling

The traditional BFM in an air quality model, which estimates the impact of the changes in specific precursor emissions on O₃ through running a scenario with only this precursor emissions varying, was recognized as the simplest source impact analysis method and has been broadly in previous researches (Chatani et al., 2020; Couzo et al., 2016; Yang et al., 1997). Though BFM owns the advantages of simple implementation and ready application, which confronts the rapidly growing computation burden when the number of control factors increases. Also, the BFM’s estimation is only representative for the scenario that is simulated if the atmospheric circumstances are highly nonlinear (Clappier et al., 2017; Cohan et al., 2005).

Hence, the DDM was proposed as a computationally efficient alternative of the BFM for the conditions of multi-scenarios calculations. DDM calculates the first-order sensitivity to a specific parameter by solving the auxiliary equations derived from the air quality model, and then estimates the single source impact based on this first-order sensitivity (Dunker, 1984). The accuracy of DDM could only be insurable for predicting the pollutant response in a linear system, but it was well known that O₃ was generated by the complex nonlinear interactions between NO_x and VOC in most cases (Cohan et al., 2005). Thus, a Higher-Order DDM (HDDM) was developed to compute the higher-order sensitivity through differentiating the governing equations of the first-order sensitivity in the CTM (Hakami et al., 2003, 2004). With the combination of the calculated first-order and higher-order sensitivities, the nonlinear impact of the changes in specific precursor emissions on O₃ can be estimated by the HDDM. The detailed calculation process of both BFM and HDDM is described in SI.

2.2.2. Source contribution modeling

The source contribution modeling technique for O₃ analysis, which mostly refers to the OSAT embedded in the CAMx that allocates the source contributions through tracking the chemical tracers (Yarwood et al., 1996). The O₃ precursors (i.e., NO_x and VOC) from each source were followed by adding the tracer families to the CAMx model, and the tracers were created where the O₃ was generated. One tracer family was

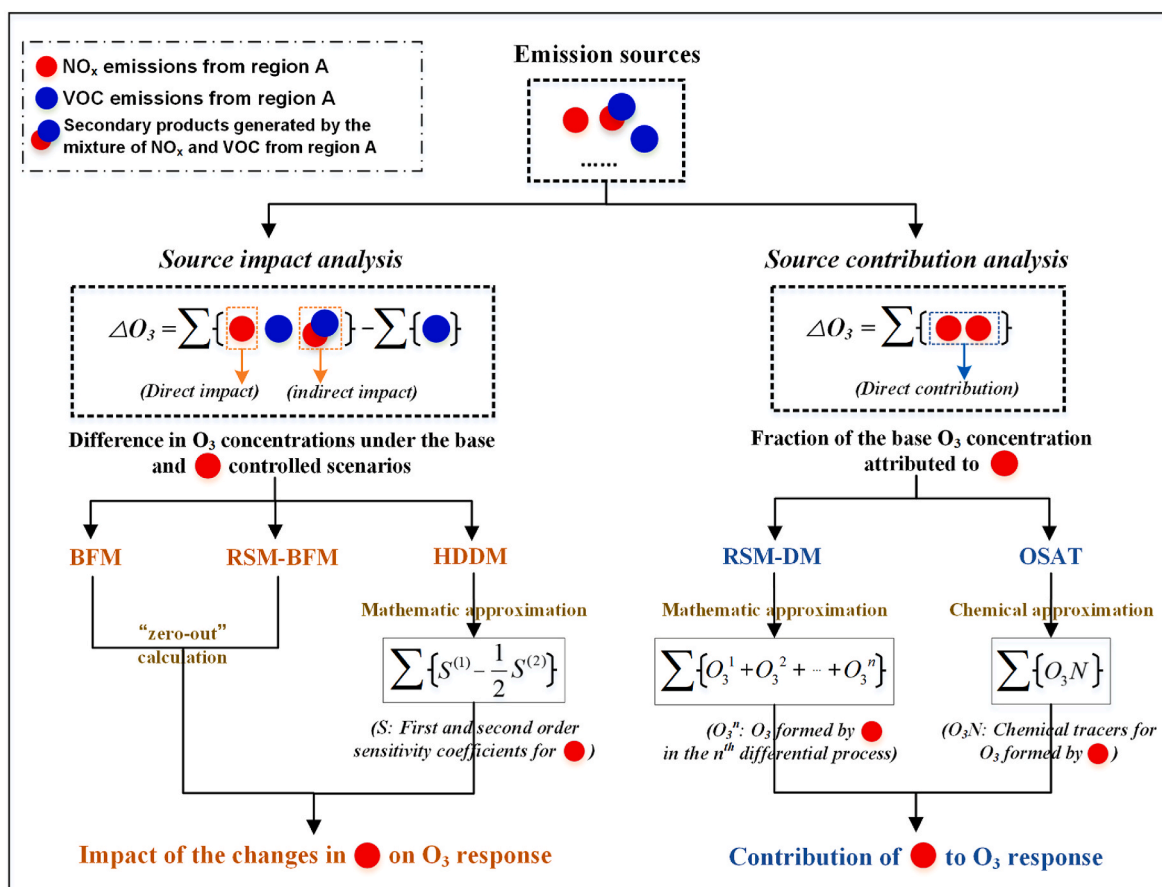


Fig. 3. Illustration of the calculation process of BFM, RSM-BFM, HDDM, RSM-DM, and OSAT for estimating the impact and contribution of an example emission source, NO_x emissions from source region A.

employed for one source group in OSAT, and each family consisted of four tracers, including the tracers for NO_x, VOC, O₃ formed by NO_x, and O₃ formed by VOC.

For determining the O₃ formation regime and allocating the contribution of each emission source to O₃, the indicator of the ratio of nitric acid (HNO₃) and hydrogen peroxide (H₂O₂) defined in former researches was adopted in this study, for which a ratio exceeded 0.35 indicated that the O₃ formation was NO_x sensitive, otherwise, it was VOC sensitive (Dunker et al., 2002; Itahashi et al., 2015). Based on the identified O₃ formation regime, the changes in O₃ concentration caused by NO_x and VOC emissions from a specific source region can be estimated for further calculation of source contributions. The detailed calculation process of OSAT is also described in SI.

2.2.3. Response surface modeling

RSMs are the meta-models derived from the CMAQ simulations, which can predict the pollutant response to any magnitude of perturbations more flexibly and efficiently compared with the traditional air quality models (USEPA, 2006). To effectively analyze the nonlinear response of air pollutants to multiregional and multisectoral source emissions, RSMs have been continuously improved using prior knowledge, such as an extended version of the original RSM (ERSM) for multiregional predictions (Xing et al., 2017; Zhao et al., 2015) and a polynomial function-based RSM (pf-RSM) for improving the capability in nonlinearity quantification (Xing et al., 2018). The integration of ERSM and pf-RSM was also recently employed by us in the case study of the PRD region, in which the relationship between the O₃ and its precursors in each source region was constructed by a series of polynomial functions (Fang et al., 2020). The development of RSM in this study is similar to that in our previous research (Fang et al., 2020), in simple

terms, there is one scenario of baseline CMAQ simulation for reference, 21 scenarios for constructing the relationship between the O₃ response in each receptor region to emission changes in each source region, 21 scenarios for establishing the relation between the O₃ response in each receptor to simultaneous emission changes in all source regions, and additional 10 scenarios for out-of-sample validation of the RSM. The validation results of RSM are detailed in SI.

Based on the established RSM, various emission source contributions to O₃ can be numerically estimated by RSM-BFM and RSM-DM. RSM-BFM is similar to the traditional BFM in an air quality model but utilizes a more flexible mathematic equation to estimate the impact of a perturbed emission source. Regarding the RSM-DM, briefly, DM computes the sum of the pollutant response to each tiny perturbation of a specific source as the contribution, which can capture the negative contribution on the one hand, and ensure that the accumulated contributions are equal to the actual O₃ response derived from the CMAQ integrated scenarios on the other hand; furthermore, a sectoral linear fitting technique (SL) in RSM was also previously proposed by us to draw the emission weight of each sector and quantify the various sectoral contributions to O₃. Descriptions about both the development of DM and SL have been detailed in our latest publication (Fang et al., 2020).

3. Results and discussion

3.1. Analysis of multiregional O₃ source impacts and contributions

3.1.1. Apportionments of source impacts and contributions

BFM, RSM-BFM, HDDM, RSM-DM, and OSAT were applied for assessing regional impacts and contributions in the case study of the PRD, and the dynamic scenarios of 25 %, 50 %, 75 %, and 100 % control

were implemented for a comprehensive analysis.

The three receptor regions (i.e., GZ, FS, and ZQ) relatively by the north of the PRD usually experience more serious O₃ pollution in September (Fig. 4), resulting from the intensive local precursor emissions, and also the transported pollutants from the areas out of the PRD brought by the prevailing north-easterly wind (Li et al., 2012). In GZ and FS, local NO_x emissions always exhibit a negative impact or contribution even under the 100 % control, which is consistently reflected in the calculations of BFM, RSM-BFM, HDDM, and RSM-DM; yet OSAT was not designed to track the O₃ depletion process and thus does not provide information about the O₃ disbenefits caused by the NO titration. In addition, it is noticed that the negative impact assessed by BFM, RSM-BFM, and HDDM is usually more obvious than the negative contribution predicted by the RSM-DM in GZ and FS. It was because in most cases, O₃ exhibited a strong nonlinear relationship with its

precursors, especially NO_x, at this time the indirect effects among two or more emission sources were found to exert a non-ignorable influence on O₃ formation. The indirect effects together with the direct impact were both included in the impacts of single source emissions by source impact methods, while the source contribution methods separated the indirect effects and mixed them with the direct impact of a single source to represent the individual source contributions (Clappier et al., 2017; Cohan et al., 2005). Therefore, the impact (either negative or positive) assessed by BFM, RSM-BFM, and HDDM will be higher than the contribution apportioned by RSM-DM and OSAT in most conditions. Besides, we notice that the impacts obtained by the HDDM are mostly lower than those computed by BFM and RSM-BFM; for example, under the 100 % control, the impact of each source to the O₃ in GZ assessed by the HDDM is 0.64–18.45 % lower than those estimated by the BFM; it was because that the stronger nonlinear chemistry under strict control

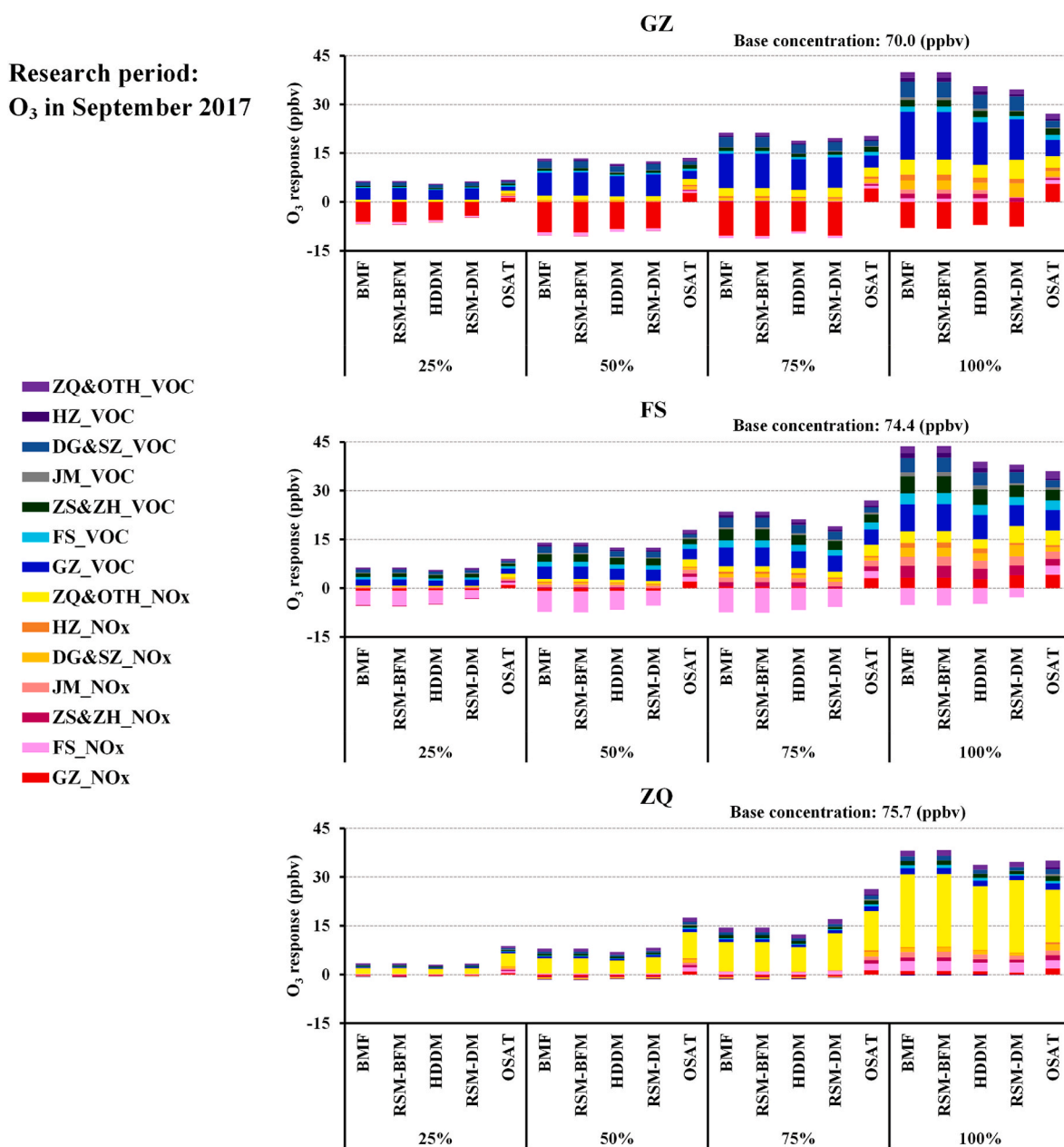


Fig. 4. Apportionments of regional O₃ source impacts (estimated by BFM, RSM-BFM, and HDDM) and source contributions (estimated by RSM-DM and OSAT) in GZ, FS, and ZQ, in September 2017. The colored bar denotes the impact or contribution of NO_x or VOC emissions from each source region. GZ: Guangzhou, FS: Foshan, ZQ: Zhaoqing, ZS&ZH: Zhongshan and Zhuhai, JM: Jiangmen, DG&SZ: Dongguan and Shenzhen, HZ: Huizhou, ZQ&OTH: Zhaoqing and all the other areas in the D3 domain.

scenarios cannot be entirely represented by the high-order sensitivity coefficients calculated by the HDDM (Itahashi et al., 2015). RSM-BFM overall reproduces the BFM's results directly obtained from the CMAQ, demonstrating that RSM-BFM may be more capable of analyzing the source impacts to an extensive extent. According to the results under the 100 % cut down scenario, the influence of ZQ&OTH_NO_x emissions on O₃ formation in GZ and FS is relatively high; while for the O₃ in ZQ, ZQ&OTH_NO_x is the most influential emission source, which can be viewed in the estimations of all the methods. Regarding the VOC, all the methods suggest that GZ_VOC dominates the local O₃ formation, and also has a great effect on the O₃ in FS; additionally, DG&SZ_VOC and ZS&ZH_VOC are found to exert a non-negligible effect on the O₃ in GZ and FS, respectively.

For the three regions (i.e., DG, SZ, and HZ) by the east of the PRD (Fig. S6), where the O₃ levels are lower than those in northern regions. In DG and SZ, the results of all the methods demonstrate that DG&SZ_VOC accounts for a visible proportion in the apportionments of source impacts and contributions, and it is also consistent for all the methods that DG&SZ_NO_x largely affect the O₃ in DG under the 100 % control; but for the negative contribution of DG&SZ_NO_x emissions to the O₃ in SZ, which is also not caught by the OSAT as that in GZ and FS. Another notable difference between the calculations of five methods is found in DG, which is that for GZ_NO_x, the impact of it computed by BFM, RSM-BFM, and HDDM is lower than the contribution of it derived

by RSM-DM and OSAT under the 100 % control; the possible reason for this difference is that the indirect effects caused a negative impact, which means that the interactions between GZ_NO_x and other emission sources may reduce the regional NO_x emissions transported to DG and then increase the O₃ concentrations, because the O₃ consumption was weakened by the reductions in regional NO_x emissions. In HZ, it is like that in ZQ, local NO_x emissions play a key role in O₃ formation as indicated by all the methods, and local VOC and ZQ&OTH_NO_x emissions are also worthy of attention for HZ.

The downwind regions in September of the PRD under the prevailing north-easterly wind, including ZS, ZH, and JM (Fig. S6), suffering from a more evident regional transportation from the northern areas in the D3 domain. In ZS, the agreement between all the methods is that local NO_x and VOC emissions account for most of the apportionments in source impacts and contributions when at a 100 % reduction, and DG&SZ_NO_x and DG&SZ_VOC also influence the O₃ in ZS to some extent; while the inconsistency is that comparing with other three techniques, OSAT gives more attention on some regional emission sources (i.e., FS_NO_x, JM_NO_x, and ZQ&OTH_NO_x). The probable reason for this inconsistency is that the third version of OSAT (OSAT3) formulation embedded within the CAMx v7.00 contained an updated technique to manage the NO_x recycling, which tended to allocate more O₃ concentrations to long-range regional transport of precursor emissions and less to local production, for the reason that the contribution from NO_x accumulated

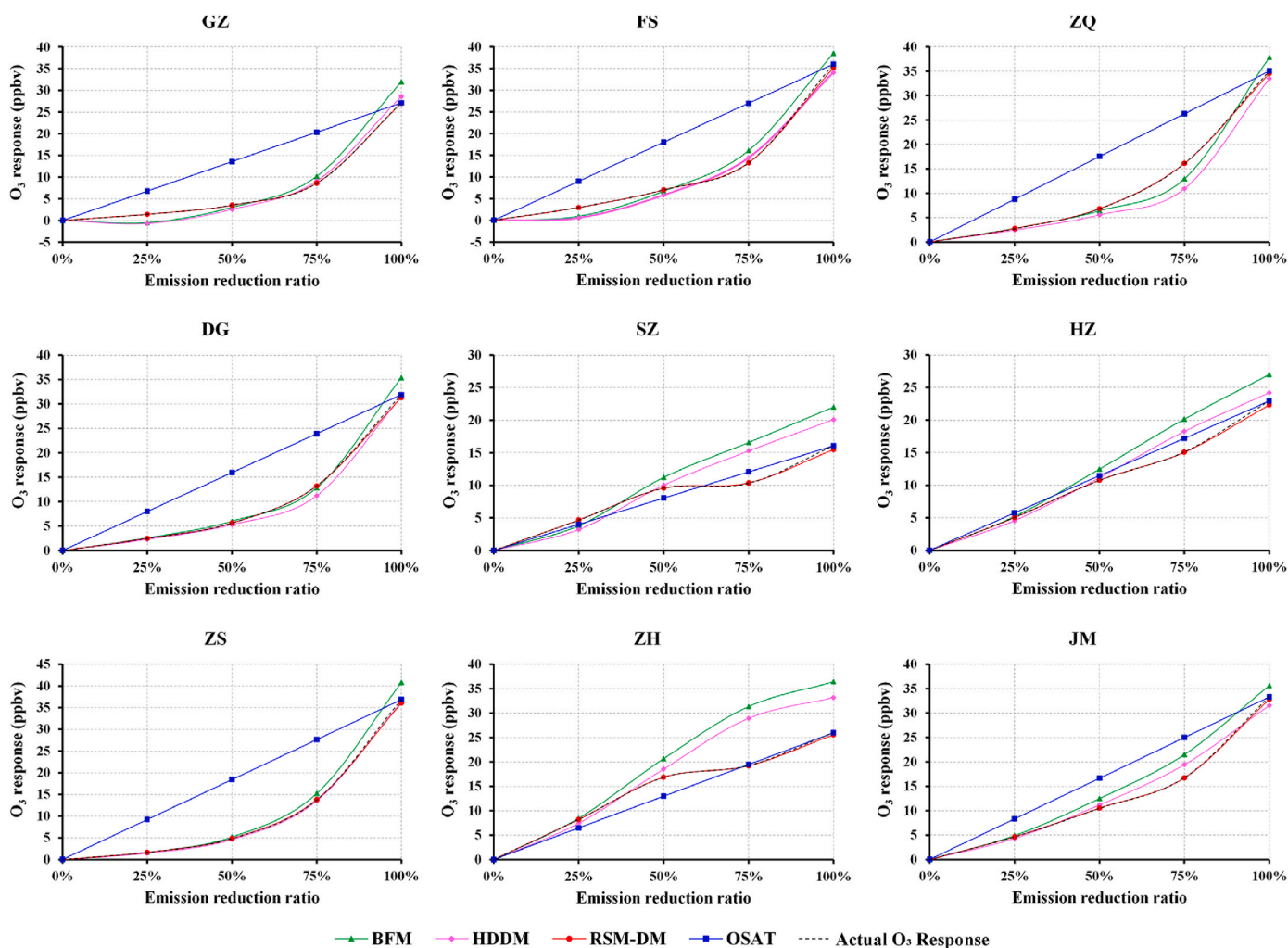


Fig. 5. Comparison of accumulative source impacts (estimated from BFM, HDDM) and source contributions (estimated from RSM-DM and OSAT) with the actual O₃ response in 9 receptor regions of the PRD, in September 2017. The actual O₃ response was derived from the CMAQ simulations under the simultaneous control of all emission sources. GZ: Guangzhou, FS: Foshan, ZQ: Zhaoqing, DG: Dongguan, SZ: Shenzhen, HZ: Huizhou, ZS: Zhongshan, ZH: Zhuhai, JM: Jiangmen.

during the downwind transport process (Price et al., 2015). In ZH and JM, the southernmost regions of the PRD, the distribution of source impacts and contributions acquired by all the methods is similar, in which the O₃ in ZH is comparably affected by NO_x and VOC emissions from ZS&ZH, DG&SZ, and GZ, while the O₃ in JM is mainly influenced by NO_x and VOC emissions from ZS&ZH and NO_x emissions from FS.

3.1.2. Accumulative source impacts and contributions

To further analyze the consistency and inconsistency between BFM, HDDM, RSM-DM, and OSAT, the accumulated source impacts and contributions in 9 receptor regions of the PRD estimated from the four methods, and the actual O₃ response directly derived from the CMAQ under the synchronous control of all emission sources were also compared together (Fig. 5). Since there was almost no difference between RSM-BFM and BFM for source impact analysis as described in Section 3.1.1, RSM-BFM was not considered for comparison in this section. As mentioned before, when the relationship between pollutant concentrations and precursor emissions is linear, the contribution of a specific emission source (individual contribution) can be viewed as the impact of this source on pollutant concentrations (individual impact), and the accumulation of individual contributions and impacts will be also equal to the actual O₃ response resulting from a simultaneous reduction of all emission sources. However, the O₃ concentrations are mostly nonlinearly response to changes in its precursors, in this case, the individual impact will not equivalent to the individual contribution because of the existence of the indirect effects, and the sum of individual source abatement impacts will be also different from the actual O₃ response resulting from a multiple source abatement scenario (Clappier et al., 2017; Cohan et al., 2005; Dunker et al., 2002; Thunis et al., 2019).

As displayed in Fig. 5, when at a 25 % emission reduction, the accumulated impacts acquired from both BFM and HDDM basically agree with the actual O₃ response in most receptors regions because of the linear responsive conditions in this time, but the disagreement is found in GZ and FS in which local NO_x emissions exert a nonlinear impact on O₃; when the emission ratio is furtherly reduced to 50 %, the accumulative impacts begin to larger than the actual O₃ response in some receptor regions (i.e., SZ, HZ, JM, and ZH), demonstrating that the O₃ concentrations are gradually nonlinearly response to precursor emissions; reinforcing the emission reduction ratio to 75 % and 100 %, the nonlinear conditions are stronger, hence the difference between the cumulative impacts and the actual O₃ response is more obvious, as exhibited by that the accumulative impacts in 9 receptor regions calculated from the BFM are about 6.99–40.17 % higher than the actual O₃ response under the 100 % control. It is also noticed that the accumulated impacts obtained from the HDDM are generally lower than those derived from the BFM; this is because, as mentioned before, HDDM can well measure the nonlinear process of O₃ formation under small or moderate control scenarios, but it exhibits obvious discrepancy compared with the BFM when strengthening the emission reduction rate to more than 50 %. For accumulated contributions obtained from the RSM-DM, they are almost equal to the actual O₃ response under different control scenarios because RSM-DM fully considers the nonlinearity (Fang et al., 2020). Concerning the OSAT, it can be seen that the variation trend of the calculated accumulative contributions under different control scenarios is linear, in which the accumulative contributions attained from the OSAT and the actual O₃ response is consistent at the 100 % emission reduction; whereas, for other conditions with the emission reduction ratio less than 100 %, OSAT is unable to ensure that the cumulative contributions agreed with the actual O₃ response because of its linear assumption.

3.1.3. Identification of top emission impact/contribution sources

While source impact and contribution analysis methods are different in their underlying algorithms, both of them can provide information about the importance of major emission sources which is of significance to support the air quality planning (Dunker et al., 2002). Therefore,

when at the 100 % emission reduction, the top-five emission sources with the most distinct impact or contribution recognized by BFM, HDDM, RSM-DM, and OSAT were selected for a comprehensive analysis (Fig. 6 and Fig. S7). It is found that there are at least two consistent sources among the top-five emission impact/contribution sources identified by all the four methods, proving that whether the source impact or source contribution methods, they are generally consistent in determining the top emission sources of importance. For example, GZ_VOC is identified as one of the top impact/contribution emission sources by all the four methods to the O₃ in GZ, with an impact/contribution of 14.7 ppbv, 13.1 ppbv, 12.5 ppbv, and 5.0 ppbv as estimated by BFM, HDDM, RSM-DM, and OSAT, respectively. In FS, the four methods are also highly consistent in identifying the top impact/contribution sources, in which GZ_VOC is the most influential emission source as discerned by all the methods, with an impact/contribution of 8.3 ppbv, 7.5 ppbv, 6.5 ppbv, and 6.3 ppbv as estimated by BFM, HDDM, RSM-DM, and OSAT, respectively. In addition, when comparing source impact methods (i.e., BFM and HDDM) and source contribution methods (i.e., RSM-DM and OSAT) separately, it is found that BFM and HDDM agree on all the top-five impact sources of O₃ in most receptor regions except the FS; although there are inconsistencies in the ranking of some factors in FS, the difference between the values is slight, suggesting that BFM and HDDM are highly consistent in providing information about the importance of major impact sources. RSM-DM and OSAT are also consistent for at least three contribution sources among the identified top-five contribution sources, and the most obvious discrepancy is also that the OSAT regarded the negative contribution source (mostly the local NO_x emissions) as the top contribution source in receptor regions existing the NO titration (i.e., GZ and SZ).

The inconsistency between source impact methods (i.e., BFM and HDDM) and source contribution methods (i.e., RSM-DM and OSAT) mostly occurs for the predictions of NO_x-related factors, in which RSM-DM and OSAT give more importance on regional NO_x emissions, especially that from GZ; for example, for O₃ in FS, DG, SZ, ZS and ZH, GZ_NO_x is regarded as one of the top-five emission sources by RSM-DM and OSAT, whereas which is not reflected in BFM and HDDM. This inconsistency possibly attributes to that the nonlinear effect of NO_x is stronger than that of the VOC on O₃ formation, hence the indirect effects of the synergy control of NO_x emissions from GZ and other source regions may be negative; in other words, the O₃ concentrations will increase because the NO titration was weakened by the simultaneous reductions in NO_x emissions from GZ and other source regions; thus the direct impact of individual source approximated by BFM and HDDM will be partially offset by this negative indirect effects, and lower than the individual source contribution.

3.2. Analysis of multisectoral O₃ source contributions

Quantification of the contributions of various emission sectors to O₃ is also of significance for policymaking, hence the apportionments of sectoral source contributions to O₃ in 9 receptor regions of the PRD were furtherly assessed by RSM-DM and OSAT. As listed in Table 1, both NO_x and VOC emissions were categorized into 4 sectors, and the contribution of each sector from each source region to O₃ was firstly analyzed as displayed in Fig. 7 and Fig. S8, then the percentage of each sectoral source contribution from the entire D3 domain was also quantified in Fig. 8.

3.2.1. Apportionments of sectoral contributions from each source region

From Fig. 7 and Fig. S8, the distribution of sectoral source contributions in each receptor region is generally similar. In GZ and FS, the largest difference is also for the contribution of local NO_x emissions, especially that from the on-road mobile source, which is negative in RSM-DM's calculations because the intensive near ground NO discharged from the vehicles can largely consume the ambient O₃, whereas OSAT also does not provide this information about the NO titration; for

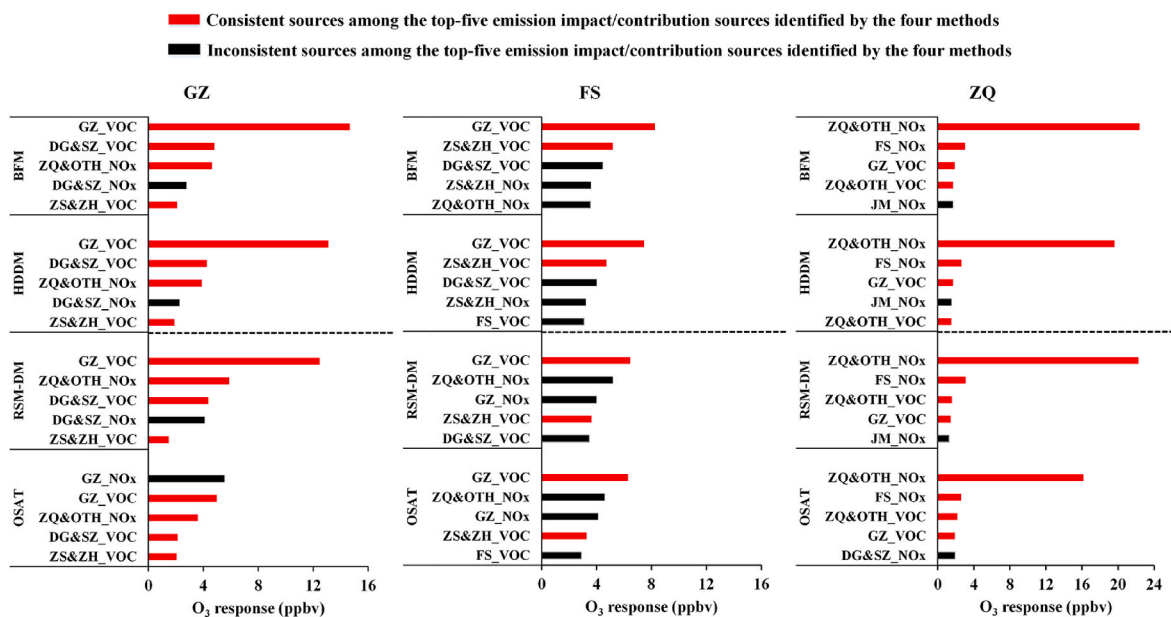


Fig. 6. Top-five emission impact/contribution sources identified by BFM, HDDM, RSM-DM, and OSAT in GZ, FS, and ZQ, in September 2017. GZ: Guangzhou, FS: Foshan, ZQ: Zhaoqing, ZS&ZH: Zhongshan and Zhuhai, JM: Jiangmen, DG&SZ: Dongguan and Shenzhen, HZ: Huizhou, ZQ&OTH: Zhaoqing and all the other areas in the D3 domain.

others NO_x emissions (i.e., industrial process and biomass burning) from ZQ&OTH, both RSM-DM and OSAT estimate a visible contribution of them to O₃ in GZ and FS; on-road mobile NO_x emissions from GZ, ZS&ZH, and DG&SZ are also observed to exhibit a non-negligible contribution to the O₃ in FS. For VOC-related emission sectors, RSM-DM and OSAT are agreed that industrial process and solvent utilization source emissions from GZ and DG&SZ exert an apparent contribution to O₃ in GZ and FS. In ZQ, on-road mobile and others NO_x emissions from ZQ&OTH dominate the O₃ generation as calculated by both RSM-DM and OSAT.

As demonstrated by Fig. S8, both RSM-DM and OSAT manifest that on-road mobile NO_x emissions, and industrial process and on-road mobile VOC emissions from DG&SZ and GZ, are of importance to O₃ formation in DG. One notable thing is that others NO_x emissions from ZQ&OTH occupy a certain amount of the contribution to the O₃ in DG according to the OSAT's results, however, which is not presented by the RSM-DM; the probable explanation for this is also the update of OSAT3 formulation in handling the NO_x recycling as mentioned in Section 3.1.1, which caused the O₃ was allocated more to long-range transport of regional NO_x emissions. About the situation in SZ, the reductions of on-road mobile NO_x emissions from DG&SZ will cause the disbenefits to O₃, and local on-road mobile VOC emissions play a key role in forming O₃ as reflected by the RSM-DM, but OSAT only estimates the slight contribution of VOC and overvalues the local on-road mobile NO_x emission contributions; for solvent utilization VOC emissions from DG&SZ, RSM-DM and OSAT are consistent for predicting its partial contribution to the O₃ in SZ. As for HZ, local on-road mobile and stationary combustion NO_x emissions are identified as major contributors by both RSM-DM and OSAT.

For the three cities (i.e., ZS, ZH, and JM) by the south of the PRD (Fig. S8), on-road mobile NO_x and VOC emissions from ZS&ZH and GZ greatly contribute to the O₃ formation in ZS. For ZH, the southernmost coastal city in the PRD, both RSM-DM and OSAT reveal that the contribution of on-road mobile NO_x emissions from ZS&ZH accounts for a relatively large proportion, and non-road mobile NO_x emissions from GZ, which are probably emitted from the southern boundary of GZ where the activities of agricultural machinery or ships are intensive, also affect the O₃ in ZH to a certain extent. In JM, according to the results of RSM-DM and OSAT, others NO_x emissions from FS, which are most

likely to be those from the biomass burning source on the border of FS and JM, exert an apparent contribution to O₃, and the contribution of on-road mobile NO_x emissions from ZS&ZH is also noteworthy for JM.

3.2.2. Apportionments of sectoral contributions from the entire D3 domain

The percentage of the contribution from each sectoral emission source within the entire D3 domain was also allocated using RSM-DM and OSAT (Fig. 8 and Table S3). What is found is that the distribution of the apportioned percentages in 9 receptor regions is generally similar except for GZ and SZ, in which for on-road mobile NO_x emissions, OSAT predicts a considerable contribution of it to O₃ formation, but RSM-DM's predictions are much lower and even negative in GZ, because that the apparent negative contribution of local on-road mobile NO_x emissions was not considered by the OSAT. In FS, DG, ZS, and JM, RSM-DM and OSAT are overall consistent for predicting the sectoral contributions, in which on-road mobile NO_x emissions are identified as the primary contributor to O₃ in DG, ZS, and JM by both RSM-DM and OSAT; while in FS, on-road mobile NO_x together with industrial process VOC emissions are the greatest contributor with a contribution ratio of 16.6 % as assessed by the OSAT, while RSM-DM gives the most importance on the contribution of on-road mobile VOC emissions with a proportion of 16.2 %, following by on-road mobile NO_x emissions with a contribution ratio of 15.6 %. In the other three cities (i.e., ZQ, HZ, and ZH), consistency between RSM-DM and OSAT is a little low, but they basically agree in recognizing two emission sectors with the largest contribution ratios, for example, NO_x emission contributions from on-road mobile and others to the O₃ in ZQ, and NO_x emission contributions from on-road mobile and stationary combustion to the O₃ in HZ; in ZH, the proportion of on-road mobile NO_x emission contributions estimated by RSM-DM and OSAT is comparable, and the difference is that the most significant sector recognized by the RSM-DM is NO_x emissions from non-road mobile and stationary combustion both with a contribution rate of 20.3 %, while OSAT has a higher estimation for the contributions of VOC-related sectoral emissions, especially those from industrial process source compared with the RSM-DM. Further, we notice that in ZQ, HZ, JM, and ZH, OSAT also pays more attention to the contributions of VOC-related emission sectors particularly industrial process VOC emissions in comparison with the RSM-DM, which may be related to that OSAT employed the specific OH reactivity to allocate the VOC emission contributions

Research period:
O₃ in September 2017

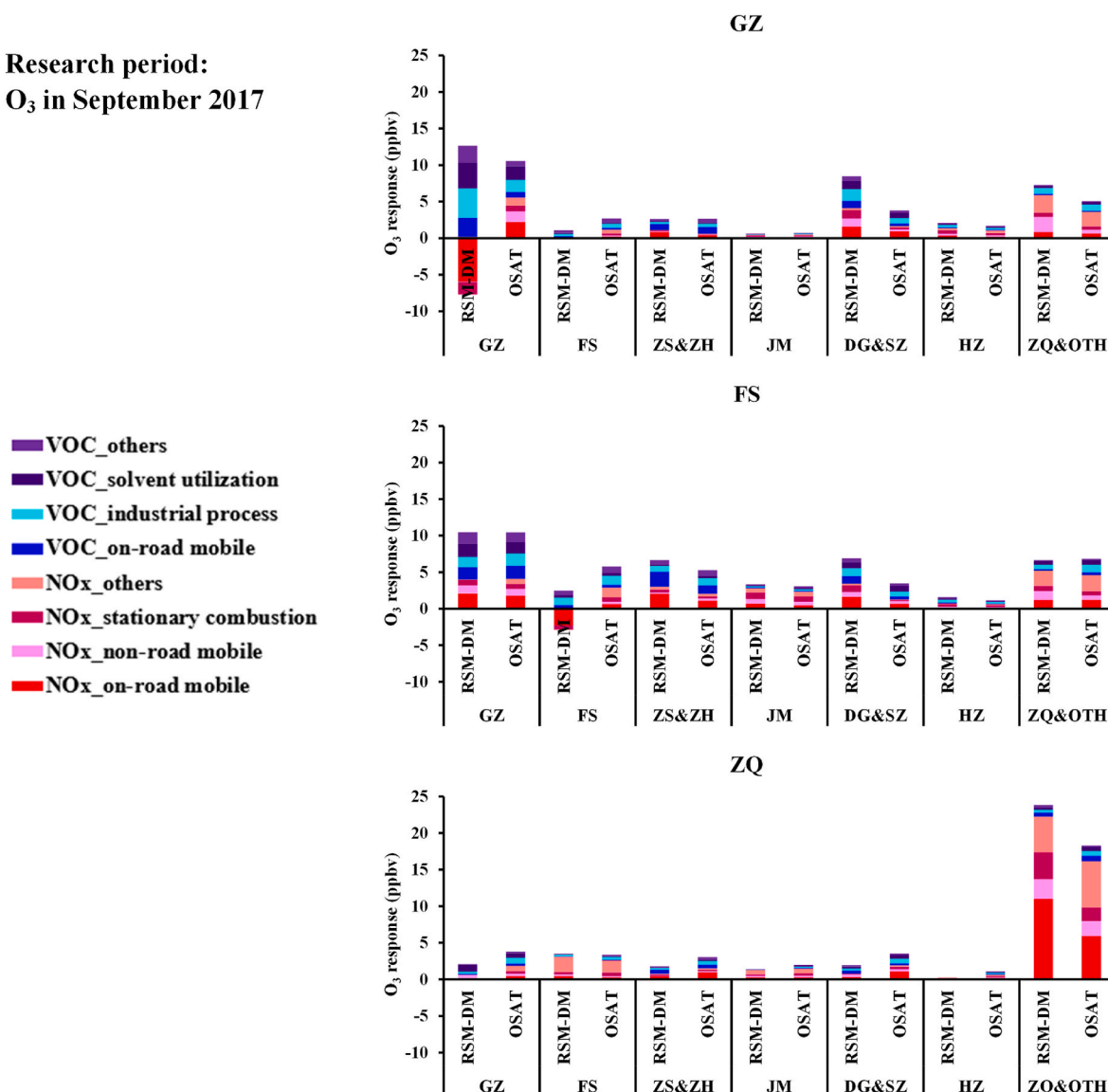


Fig. 7. Apportionments of sectoral contributions from each source region to O₃ in GZ, FS, and ZQ estimated by RSM-DM and OSAT, in September 2017. The horizontal text at the x-axis denotes the source region; the colored bar denotes the source contribution of NO_x or VOC emissions from each sector in the corresponding source region. GZ: Guangzhou, FS: Foshan, ZQ: Zhaoqing, ZS&ZH: Zhongshan and Zhuhai, JM: Jiangmen, DG&SZ: Dongguan and Shenzhen, HZ: Huizhou, ZQ&OTH: Zhaoqing and all the other areas in the D3 domain.

from different sectors to O₃, but RSM-DM relied on the emission weight of each sector to numerically apportion the corresponding source contribution. In general, RSM-DM and OSAT agree that on-road mobile (including both NO_x and VOC emissions) and industrial process (mainly VOC emissions) sources were the main contribution sectors in the PRD, contributing an average of 31.5 % and 11.4 % (estimated by RSM-DM) and 29.2 % and 13.0 % (estimated by OSAT) respectively to O₃ formation in 9 receptor regions of the PRD.

4. Conclusions

In this study, O₃ source impacts and contributions in the PRD region of China were comprehensively analyzed using multiple modeling approaches, namely BFM, RSM-BFM, HDDM, RSM-DM, and OSAT. All five methods were utilized for analyzing source impacts and contributions of NO_x and VOC emitted from multiple source regions, and RSM-DM and OSAT were selected for further analysis of NO_x and VOC emission contributions from multiple sectors in multiple source regions.

The multi-modeling evaluation results implied that due to the

nonlinearity of O₃ response to emission reductions in its precursors, particularly NO_x, source impact methods may not be applicable to apportion the contributions of various source emissions to O₃, and source contribution methods were also inappropriate to assess the impacts of emission changes on O₃. It was because that the nonlinear atmospheric conditions usually existed with the indirect effects (defined as the effects of multi-source interactions on O₃). The indirect effects together with the direct impact of a single source were both included in the impacts of individual source emissions by source impact analysis methods, while the source contribution methods separated the indirect effects and mixed them with the direct impact to represent the individual source contributions, causing the difference between source contributions and source impacts. Accordingly, under the typical nonlinear atmospheric conditions during the O₃ formation, BFM, RSM-BFM, and HDDM seemed to be appropriate for single source impact assessments to support the air quality planning, in which RSM-BFM can reproduce the BFM results derived from the CMAQ simulations, but the results of HDDM could deviate from those of BFM under moderate or strict control scenarios in which the emission reduction ratio was more

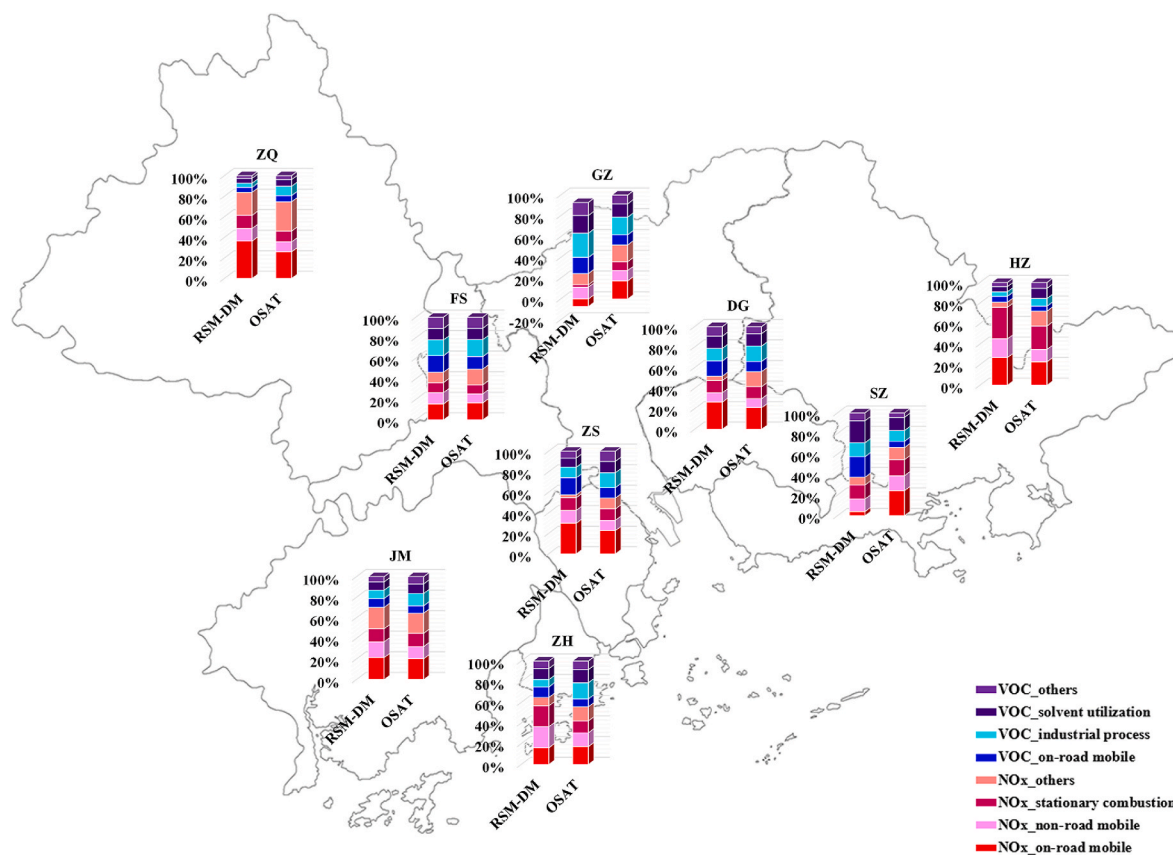


Fig. 8. Apportionments of the percentage of each sectoral contribution from the entire D3 domain to O_3 in 9 receptor regions of the PRD estimated by RSM-DM and OSAT, in September 2017. GZ: Guangzhou, FS: Foshan, ZQ: Zhaoqing, DG: Dongguan, SZ: Shenzhen, HZ: Huizhou, ZS: Zhongshan, ZH: Zhuhai, JM: Jiangmen.

than 50 %. Under multi-source control scenarios, both RSM-DM and OSAT can be reasonably applied for apportioning the various source contributions to O_3 concentrations, whereas OSAT had the limitation of representing the nonlinear response of O_3 to emission changes in its precursor (e.g., O_3 disbenefits due to local NO_x emission reductions in major cities). RSM-DM was demonstrated to be able to well capture the nonlinear negative contribution of local NO_x emission reductions to O_3 in major cities (e.g., GZ and FS) of the PRD, and ensured that the accumulated contributions were agreed with the actual O_3 response simulated by the CMAQ under the integrated control scenarios. Besides, despite source impact and source contribution methods exhibited different principles and applicability, they can generally derive similar information about the top emission sources of importance as shown in this study.

The source contribution results obtained by RSM-DM and OSAT manifested that on-road mobile (including both NO_x and VOC emissions) and industrial process (mainly VOC emissions) sources were two major contribution sectors in the PRD, with an average contribution of 31.5 % and 11.4 % (estimated by RSM-DM) and 29.2 % and 13.0 % (estimated by OSAT) respectively to O_3 formation in 9 receptor regions of the PRD. Consequently, the strengthened controls on NO_x and VOC emissions from on-road mobile and industrial process sources in the central cities (i.e., GZ, FS, DG&SZ, and ZS) of PRD are recommended for policymakers to effectively moderate the O_3 pollution over the PRD.

Credit author statement

Tingting Fang: Conceptualization, Methodology, Modeling, Software, Investigation, Writing - Original Draft. Yun Zhu: Resources, Writing - Review & Editing, Supervision, Project administration, Data Curation. Shuxiao Wang: Resources, Writing - Review & Editing, Data

Curation. Jia Xing: Resources, Writing - Review & Editing, Data Curation. Bin Zhao: Writing - Review & Editing. Shaojia Fan: Writing - Review & Editing. Minhui Li: Writing - Review & Editing. Wenwei Yang: Validation, Formal analysis, Visualization, Software. Ying Chen: Validation, Formal analysis, Visualization, Modeling. Ruolin Huang: Validation, Formal analysis, Visualization, Software.

Declaration of competing interest

The authors declare that they have no known competing financial interests or personal relationships that could have appeared to influence the work reported in this paper.

Acknowledgments

This work was supported by the Science and Technology Program of Guangzhou, China (No. 202002030188), the Innovation Group Project of Southern Marine Science and Engineering Guangdong Laboratory (Zhuhai) (No. 311021001). The authors sincerely thank James T. Kelly (U.S. Environmental Protection Agency) and Carey Jang (U.S. Environmental Protection Agency) for their assistance in preparation and management of this paper. The views expressed in this paper are those of the authors alone and do not necessarily reflect the views and policies of the U.S. Environmental Protection Agency.

Appendix A. Supplementary data

Supplementary data to this article can be found online at <https://doi.org/10.1016/j.envpol.2021.117860>.

References

- U.S. EPA, 2006. Technical support document for the proposed PM NAAQS rule: response surface modeling. In: R. T. P. Office of Air Quality Planning and Standards, NC. https://www.epa.gov/sites/production/files/2020-10/documents/pmnaaqs_tsd_rm_all_021606.pdf.
- Baker, K.R., Kelly, J.T., 2014. Single source impacts estimated with photochemical model source sensitivity and apportionment approaches. *Atmos. Environ.* 96, 266–274. <https://doi.org/10.1016/j.atmosenv.2014.07.042>.
- Burr, M.J., Zhang, Y., 2011a. Source apportionment of fine particulate matter over the Eastern U.S. Part I: source sensitivity simulations using CMAQ with the Brute Force method. *Atmos. Pollut. Res.* 2 (3), 300–317. <https://doi.org/10.5094/apr.2011.036>.
- Burr, M.J., Zhang, Y., 2011b. Source apportionment of fine particulate matter over the Eastern U.S. Part II: source apportionment simulations using CAMx/PSAT and comparisons with CMAQ source sensitivity simulations. *Atmos. Pollut. Res.* 2 (3), 318–336. <https://doi.org/10.5094/apr.2011.037>.
- Byun, D., Schere, K.L., 2006. Review of the governing equations, computational algorithms, and other components of the models-3 Community Multiscale Air Quality (CMAQ) modeling system. *Appl. Mech. Rev.* 59 (1–6), 51–77. <https://doi.org/10.1115/1.2128636>.
- Chatani, S., Shimadera, H., Itahashi, S., Yamaji, K., 2020. Comprehensive analyses of source sensitivities and apportionments of PM_{2.5} and ozone over Japan via multiple numerical techniques. *Atmos. Chem. Phys.* 20 (17), 10311–10329. <https://doi.org/10.5194/acp-20-10311-2020>.
- Chen, X., Situ, S.P., Zhang, Q., Wang, X.M., Sha, C.Y., Zhou, L.Y., Wu, L.Q., Wu, L.L., Ye, L.M., Li, C., 2019. The synergetic control of NO₂ and O₃ concentrations in a manufacturing city of southern China. *Atmos. Environ.* 201, 402–416. <https://doi.org/10.1016/j.atmosenv.2018.12.021>.
- Clappier, A., Belis, C.A., Pernigotti, D., Thunis, P., 2017. Source apportionment and sensitivity analysis: two methodologies with two different purposes. *Geosci. Model Dev. (GMD)* 10 (11), 4245–4256. <https://doi.org/10.5194/gmd-10-4245-2017>.
- Cohan, D.S., Hakami, A., Hu, Y.T., Russell, A.G., 2005. Nonlinear response of ozone to Emissions: source apportionment and sensitivity analysis. *Environ. Sci. Technol.* 39 (17), 6739–6748. <https://doi.org/10.1021/es048664m>.
- Collet, S., Kidokoro, T., Karamchandani, P., Shah, T., Jung, J., 2017. Future-year ozone prediction for the United States using updated models and inputs. *J. Air Waste Manag. Assoc.* 67 (8), 938–948. <https://doi.org/10.1080/10962247.2017.1310149>.
- Collet, S., Kidokoro, T., Karamchandani, P., Jung, J., Shah, T., 2018. Future year ozone source attribution modeling study using CMAQ-ISAM. *J. Air Waste Manag. Assoc.* 68 (11), 1239–1247. <https://doi.org/10.1080/10962247.2018.1496954>.
- Couzo, E., McCann, J., Vizuete, W., Blumsack, S., West, J.J., 2016. Modeled response of ozone to electricity generation emissions in the northeastern United States using three sensitivity techniques. *J. Air Waste Manag. Assoc.* 66 (5), 456–469. <https://doi.org/10.1080/10962247.2016.1143412>.
- DEPGP, 2020. 2019 Report on the State of Guangdong Provincial Environment. http://gdee.gd.gov.cn/hjzqgb/content/post_3007132.html.
- Dolwick, P., Akhtar, F., Baker, K.R., Possiel, N., Simon, H., Tonnesen, G., 2015. Comparison of background ozone estimates over the western United States based on two separate model methodologies. *Atmos. Environ.* 109, 282–296. <https://doi.org/10.1016/j.atmosenv.2015.01.005>.
- Dunker, A.M., 1984. The decoupled direct method for calculating sensitivity coefficients in chemical kinetics. *J. Chem. Phys.* 81 (5), 2385–2393. <https://doi.org/10.1063/1.447938>.
- Dunker, A.M., Yarwood, G., Ortman, J.P., Wilson, G.M., 2002. Comparison of source apportionment and source sensitivity of ozone in a three-dimensional air quality model. *Environ. Sci. Technol.* 36 (13), 2953–2964. <https://doi.org/10.1021/es011418f>.
- Fang, T.T., Zhu, Y., Jang, J.C., Wang, S.X., Xing, J., Chiang, P.-C., Fan, S.J., You, Z.Q., Li, J.Y., 2020. Real-time source contribution analysis of ambient ozone using an enhanced meta-modeling approach over the Pearl River Delta Region of China. *J. Environ. Manag.* 268. <https://doi.org/10.1016/j.jenvman.2020.110650>.
- Feng, Z.Z., Hu, E.Z., Wang, X.K., Jiang, L.J., Liu, X.J., 2015. Ground-level O₃ pollution and its impacts on food crops in China: a review. *Environ. Pollut.* 199, 42–48. <https://doi.org/10.1016/j.envpol.2015.01.016>.
- Foley, K.M., Roselle, S.J., Appel, K.W., Bhavsar, P.V., Pleim, J.E., Otte, T.L., Mathur, R., Sarwar, G., Young, J.O., Gilliam, R.C., Nolte, C.G., Kelly, J.T., Gilliland, A.B., Bash, J.O., 2010. Incremental testing of the Community Multiscale Air Quality (CMAQ) modeling system version 4.7. *Geosci. Model Dev. (GMD)* 3 (1), 205–226. <https://doi.org/10.5194/gmd-3-205-2010>.
- Gao, M., Gao, J.H., Zhu, B., Kumar, R., Lu, X., Song, S.J., Zhang, Y.Z., Jia, B.X., Wang, P., Beig, G.R., Hu, J.L., Ying, Q., Zhang, H.L., Sherman, P., McElroy, M.B., 2020. Ozone pollution over China and India: seasonality and sources. *Atmos. Chem. Phys.* 20 (7), 4399–4414. <https://doi.org/10.5194/acp-20-4399-2020>.
- Ge, S.J., Wang, S.J., Xu, Q., Ho, T., 2021. Source apportionment simulations of ground-level ozone in Southeast Texas employing OSAT/APCA in CAMx. *Atmos. Environ.* 253, 118370. <https://doi.org/10.1016/j.atmosenv.2021.118370>.
- Gong, X., Hong, S., Jaffe, D.A., 2018. Ozone in China: spatial distribution and leading meteorological factors controlling O₃ in 16 Chinese cities. *Aerosol. Air Qual. Res.* 18 (9), 2287–2300. <https://doi.org/10.4209/aaqr.2017.10.0368>.
- Grulke, N.E., Heath, R.L., 2020. Ozone effects on plants in natural ecosystems. *Plant Biol.* 22, 12–37. <https://doi.org/10.1111/plb.12971>.
- Hakami, A., Odman, M.T., Russell, A.G., 2003. High-order, direct sensitivity analysis of multidimensional air quality models. *Environ. Sci. Technol.* 37 (11), 2442–2452. <https://doi.org/10.1021/es020677h>.
- Hakami, A., Odman, M.T., Russell, A.G., 2004. Nonlinearity in atmospheric response: a direct sensitivity analysis approach. *J. Geophys. Res. Atmos.* 109 (D15). <https://doi.org/10.1029/2003jd004502>.
- Hallquist, M., Munthe, J., Hu, M., Wang, T., Chan, C.K., Gao, J., Boman, J., Guo, S., Hallquist, A.M., Mellqvist, J., Moldanova, J., Pathak, R.K., Pettersson, J.B.C., Pleijel, H., Simpson, D., Thynell, M., 2016. Photochemical smog in China: scientific challenges and implications for air-quality policies. *Natl. Sci. Rev.* 3 (4), 401–403. <https://doi.org/10.1093/nsr/nww080>.
- Han, X., Zhu, L.Y., Wang, S.L., Meng, X.Y., Zhang, M.G., Hu, J., 2018. Modeling study of impacts on surface ozone of regional transport and emissions reductions over North China Plain in summer 2015. *Atmos. Chem. Phys.* 18 (16), 12207–12221. <https://doi.org/10.5194/acp-18-12207-2018>.
- HKEPD, 2017. Pearl River Delta Regional Air Quality Monitoring Report for Year 2017. https://www.epd.gov.hk/epd/sites/default/files/epd/english/resources/pub/publications/files/PRD_2017_report_en.pdf.
- Huang, S.J., Hu, Y.T., Zheng, J.Y., Yuan, Z.B., Russell, A.G., Ou, J.M., Zhong, Z.M., 2017. A new combined stepwise-based high-order decoupled direct and reduced-form method to improve uncertainty analysis in PM_{2.5} simulations. *Environ. Sci. Technol.* 51 (7), 3852–3859. <https://doi.org/10.1021/acs.est.6b05479>.
- Itahashi, S., Uno, I., Kim, S., 2013. Seasonal source contributions of tropospheric ozone over East Asia based on CMAQ-HDDM. *Atmos. Environ.* 70, 204–217. <https://doi.org/10.1016/j.atmosenv.2013.01.026>.
- Itahashi, S., Hayami, H., Uno, I., 2015. Comprehensive study of emission source contributions for tropospheric ozone formation over East Asia. *J. Geophys. Res.* Atmos. 120 (1), 331–358. <https://doi.org/10.1002/2014jd022117>.
- Itahashi, S., Mathur, R., Hogrefe, C., Napelenok, S.L., Zhang, Y., 2020. Modeling stratospheric intrusion and trans-Pacific transport on tropospheric ozone using hemispheric CMAQ during April 2010-Part 2: examination of emission impacts based on the higher-order decoupled direct method. *Atmos. Chem. Phys.* 20 (6), 3397–3413. <https://doi.org/10.5194/acp-20-3397-2020>.
- Jin, J.B., Zhu, Y., Jang, J.C., Wang, S.X., Xing, J., Chiang, P.C., Fan, S.J., Long, S.C., 2020. Enhancement of the polynomial functions response surface model for real-time analyzing ozone sensitivity. *Front. Environ. Sci. Eng.* 15 (2). <https://doi.org/10.1007/s11783-020-1323-0>.
- Kim, E., Kim, B.U., Kim, H.C., Kim, S., 2017. The variability of ozone sensitivity to anthropogenic emissions with biogenic emissions modeled by MEGAN and BEIS3. *Atmosphere* 8 (10). <https://doi.org/10.3390/atmos8100187>.
- Koo, B., Wilson, G.M., Morris, R.E., Dunker, A.M., Yarwood, G., 2009. Comparison of source apportionment and sensitivity analysis in a particulate matter air quality model. *Environ. Sci. Technol.* 43 (17), 6669–6675. <https://doi.org/10.1021/es9008129>.
- Kwok, R.H.F., Baker, K.R., Napelenok, S.L., Tonnesen, G.S., 2015. Photochemical grid model implementation and application of VOC, NO_x, and O₃ source apportionment. *Geosci. Model Dev. (GMD)* 8 (1), 99–114. <https://doi.org/10.5194/gmd-8-99-2015>.
- Li, J.Y., Huang, X., 2019a. Ground-Level ozone concentration and landscape patterns in China's urban areas. *Photogramm. Eng. Rem. Sens.* 85 (2), 145–152. <https://doi.org/10.14358/pers.85.2.145>.
- Li, Y., Lau, A.K.H., Fung, J.C.H., Zheng, J.Y., Zhong, L.J., Louie, P.K.K., 2012. Ozone source apportionment (OSAT) to differentiate local regional and super-regional source contributions in the Pearl River Delta region, China. *J. Geophys. Res. Atmos.* 117. <https://doi.org/10.1029/2011jd017340>.
- Li, L., An, J.Y., Shi, Y.Y., Zhou, M., Yan, R.S., Huang, C., Wang, H.L., Lou, S.R., Wang, Q., Lu, Q., Wu, J., 2016. Source apportionment of surface ozone in the Yangtze River Delta, China in the summer of 2013. *Atmos. Environ.* 144, 194–207. <https://doi.org/10.1016/j.atmosenv.2016.08.076>.
- Li, K., Jacob, D.J., Liao, H., Shen, L., Zhang, Q., Bates, K.H., 2019. Anthropogenic drivers of 2013–2017 trends in summer surface ozone in China. *Proc. Natl. Acad. Sci. U.S.A.* 116 (2), 422–427. <https://doi.org/10.1073/pnas.1812168116>.
- Liu, H., Liu, S., Xue, B.R., Lv, Z.F., Meng, Z.H., Yang, X.F., Xue, T., Yu, Q., He, K.B., 2018. Ground-level ozone pollution and its health impacts in China. *Atmos. Environ.* 173, 223–230. <https://doi.org/10.1016/j.atmosenv.2017.11.014>.
- Liu, H.L., Zhang, M.G., Han, X., Li, J.L., Chen, L., 2019. Episode analysis of regional contributions to tropospheric ozone in Beijing using a regional air quality model. *Atmos. Environ.* 199, 299–312. <https://doi.org/10.1016/j.atmosenv.2018.11.044>.
- Liu, R.Y., Ma, Z.W., Liu, Y., Shao, Y.C., Zhao, W., Bi, J., 2020. Spatiotemporal distributions of surface ozone levels in China from 2005 to 2017: a machine learning approach. *Environ. Int.* 142. <https://doi.org/10.1016/j.envint.2020.105823>.
- Lu, X.C., Yao, T., Li, Y., Fung, J.C.H., Lau, A.K.H., 2016. Source apportionment and health effect of NO_x over the Pearl River Delta region in southern China. *Environ. Pollut.* 212, 135–146. <https://doi.org/10.1016/j.envpol.2016.01.056>.
- Luecken, D.J., Napelenok, S.L., Strum, M., Scheffe, R., Phillips, S., 2018. Sensitivity of ambient atmospheric formaldehyde and ozone to precursor species and source types across the United States. *Environ. Sci. Technol.* 52 (8), 4668–4675. <https://doi.org/10.1021/acs.est.7b05509>.
- Moghani, M., Archer, C.L., Mirzakhilali, A., 2018. The importance of transport to ozone pollution in the US Mid-Atlantic. *Atmos. Environ.* 191, 420–431. <https://doi.org/10.1016/j.atmosenv.2018.08.005>.
- Pan, Y.Z., Zhu, Y., Jang, J.C., Wang, S.X., Xing, J., Chiang, P.-C., Zhao, X.T., You, Z.Q., Yuan, Y.Z., 2020. Source and sectoral contribution analysis of PM_{2.5} based on efficient response surface modeling technique over Pearl River Delta Region of China. *Sci. Total Environ.* 737. <https://doi.org/10.1016/j.scitotenv.2020.139655>.
- Price, J., Yarwood, G., Koo, B., 2015. Final report improved OSAT, APCA and PSAT algorithms for CAMx. Contract 582, 15–50417.
- Shen, L., Jacob, D.J., Liu, X., Huang, G.Y., Li, K., Liao, H., Wang, T., 2019. An evaluation of the ability of the Ozone Monitoring Instrument (OMI) to observe boundary layer

- ozone pollution across China: application to 2005–2017 ozone trends. *Atmos. Chem. Phys.* 19 (9), 6551–6560. <https://doi.org/10.5194/acp-19-6551-2019>.
- Shu, L., Wang, T.J., Han, H., Xie, M., Chen, P.L., Li, M.M., Wu, H., 2020. Summertime ozone pollution in the Yangtze River Delta of eastern China during 2013–2017: synoptic impacts and source apportionment. *Environ. Pollut.* 257 <https://doi.org/10.1016/j.envpol.2019.113631>.
- Stockwell, W.R., Saunders, E., Goliff, W.S., Fitzgerald, R.M., 2020. A perspective on the development of gas-phase chemical mechanisms for Eulerian air quality models. *J. Air Waste Manag. Assoc.* 70 (1), 44–70. <https://doi.org/10.1080/10962247.2019.1694605>.
- Thunis, P., Clappier, A., Tarrason, L., Cuvelier, C., Monteiro, A., Pisoni, E., Wesseling, J., Belisa, C.A., Pirovano, G., Janssen, S., Guerreiro, C., Peduzzi, E., 2019. Source apportionment to support air quality planning: strengths and weaknesses of existing approaches. *Environ. Int.* 130 <https://doi.org/10.1016/j.envint.2019.05.019>.
- U.S. EPA, 2020. Integrated Science Assessment (ISA) for Ozone and Related Photochemical Oxidants (Final Report, Apr 2020). W. U.S. Environmental Protection Agency, DC. EPA/600/R-20/012. <https://cfpub.epa.gov/ncea/isa/recordisplay.cfm?deid=348522>.
- Wang, X.S., Li, J.L., Zhang, Y.H., Xie, S.D., Tang, X.Y., 2009. Ozone source attribution during a severe photochemical smog episode in Beijing, China. *Sci. China. [B]-Chem.* 52 (8), 1270–1280. <https://doi.org/10.1007/s11426-009-0137-5>.
- Wang, S.X., Xing, J., Jang, C.R., Zhu, Y., Fu, J.S., Hao, J.M., 2011a. Impact assessment of ammonia emissions on inorganic aerosols in east China using response surface modeling technique. *Environ. Sci. Technol.* 45 (21), 9293–9300. <https://doi.org/10.1021/es2022347>.
- Wang, X.S., Zhang, Y.H., Hu, Y.T., Zhou, W., Zeng, L.M., Hu, M., Cohan, D.S., Russell, A. G., 2011b. Decoupled direct sensitivity analysis of regional ozone pollution over the Pearl River Delta during the PRIDE-PRD2004 campaign. *Atmos. Environ.* 45 (28), 4941–4949. <https://doi.org/10.1016/j.atmosenv.2011.06.006>.
- Wang, S.X., Zhao, B., Cai, S.Y., Klimont, Z., Nielsen, C.P., Morikawa, T., Woo, J.H., Kim, Y., Fu, X., Xu, J.Y., Hao, J.M., He, K.B., 2014. Emission trends and mitigation options for air pollutants in East Asia. *Atmos. Chem. Phys.* 14 (13), 6571–6603. <https://doi.org/10.5194/acp-14-6571-2014>.
- Wang, N., Lyu, X.P., Deng, X.J., Huang, X., Jiang, F., Ding, A.J., 2019. Aggravating O₃ pollution due to NO_x emission control in eastern China. *Sci. Total Environ.* 677, 732–744. <https://doi.org/10.1016/j.scitotenv.2019.04.388>.
- Wu, Z.Y., Zhang, Y.Q., Zhang, L.M., Huang, M.J., Zhong, L.J., Chen, D.H., Wang, X.M., 2019. Trends of outdoor air pollution and the impact on premature mortality in the Pearl River Delta region of southern China during 2006–2015. *Sci. Total Environ.* 690, 248–260. <https://doi.org/10.1016/j.scitotenv.2019.06.401>.
- Xing, J., Wang, S.X., Jang, C., Zhu, Y., Hao, J.M., 2011. Nonlinear response of ozone to precursor emission changes in China: a modeling study using response surface methodology. *Atmos. Chem. Phys.* 11 (10), 5027–5044. <https://doi.org/10.5194/acp-11-5027-2011>.
- Xing, J., Wang, S.X., Zhao, B., Wu, W.J., Ding, D.A., Jang, C., Zhu, Y., Chang, X., Wang, J. D., Zhang, F.F., Hao, J.M., 2017. Quantifying nonlinear multiregional contributions to ozone and fine particles using an updated response surface modeling technique. *Environ. Sci. Technol.* 51 (20), 11788–11798. <https://doi.org/10.1021/acs.est.7b01975>.
- Xing, J., Ding, D., Wang, S.X., Zhao, B., Jang, C., Wu, W.J., Zhang, F.F., Zhu, Y., Hao, J. M., 2018. Quantification of the enhanced effectiveness of NO_x control from simultaneous reductions of VOC and NH₃ for reducing air pollution in the Beijing-Tianjin-Hebei region, China. *Atmos. Chem. Phys.* 18 (11), 7799–7814. <https://doi.org/10.5194/acp-18-7799-2018>.
- Xing, J., Ding, D., Wang, S.X., Dong, Z.X., Kelly, J.T., Jang, C., Zhu, Y., Hao, J.M., 2019. Development and application of observable response indicators for design of an effective ozone and fine-particle pollution control strategy in China. *Atmos. Chem. Phys.* 19 (21), 13627–13646. <https://doi.org/10.5194/acp-19-13627-2019>.
- Xing, J., Li, S.W., Jiang, Y.Q., Wang, S.X., Ding, D., Dong, Z.X., Zhu, Y., Hao, J.M., 2020a. Quantifying the emission changes and associated air quality impacts during the COVID-19 pandemic on the North China Plain: a response modeling study. *Atmos. Chem. Phys.* 20 (22), 14347–14359. <https://doi.org/10.5194/acp-20-14347-2020>.
- Xing, J., Zheng, S.X., Ding, D., Kelly, J.T., Wang, S.X., Li, S.W., Qin, T., Ma, M.Y., Dong, Z.X., Jang, C., Zhu, Y., Zheng, H.T., Ren, L., Liu, T.Y., Hao, J.M., 2020b. Deep learning for prediction of the air quality response to emission changes. *Environ. Sci. Technol.* 54 (14), 8589–8600. <https://doi.org/10.1021/acs.est.0c02923>.
- Yang, Y.J., Wilkinson, J.G., Russell, A.G., 1997. Fast, direct sensitivity analysis of multidimensional photochemical models. *Environ. Sci. Technol.* 31 (10), 2859–2868. <https://doi.org/10.1021/es970117w>.
- Yang, X.Y., Wu, K., Lu, Y.Q., Wang, S.G., Qiao, Y.H., Zhang, X.L., Wang, Y.R., Wang, H.L., Liu, Z.H., Liu, Y.L., Lei, Y., 2021. Origin of regional springtime ozone episodes in the Sichuan Basin, China: role of synoptic forcing and regional transport. *Environ. Pollut.* 278 <https://doi.org/10.1016/j.envpol.2021.116845>, 116845–116845.
- Yarwood, G., Morris, R.E., Yocke, M.A., Hogo, H., Chico, T., 1996. Development of a Methodology for Source Apportionment of Ozone Concentration Estimates from a Photochemical Grid Model. Paper Presented at the Proceedings of the 1996 Air & Waste Management Association's 89th Annual Meeting & Exhibition, June 23, 1996 - June 28, Nashville, TN, USA, 1996.
- Yarwood, G., Jung, J., Whitten, G.Z., Heo, G., Mellberg, J., Estes, M., 1997. UPDATES TO THE CARBON BOND MECHANISM FOR VERSION 6 (CB6).
- You, Z.Q., Zhu, Y., Jang, C., Wang, S.X., Gao, J., Lin, C.-J., Li, M.H., Zhu, Z.H., Wei, H., Yang, W.W., 2017. Response surface modeling-based source contribution analysis and VOC emission control policy assessment in a typical ozone-polluted urban Shunde, China. *J. Environ. Sci. (China)* 51, 294–304. <https://doi.org/10.1016/j.jes.2016.05.034>.
- Zhang, W., Capps, S.L., Hu, Y., Nenes, A., Napelenok, S.L., Russell, A.G., 2012. Development of the high-order decoupled direct method in three dimensions for particulate matter: enabling advanced sensitivity analysis in air quality models. *Geosci. Model Dev. (GMD)* 5 (2), 355–368. <https://doi.org/10.5194/gmd-5-355-2012>.
- Zhang, R., Cohan, A., Biazar, A.P., Cohan, D.S., 2017. Source apportionment of biogenic contributions to ozone formation over the United States. *Atmos. Environ.* 164, 8–19. <https://doi.org/10.1016/j.atmosenv.2017.05.044>.
- Zhao, B., Wang, S.X., Xing, J., Fu, K., Fu, J.S., Jang, C., Zhu, Y., Dong, X.Y., Gao, Y., Wu, W.J., Wang, J.D., Hao, J.M., 2015. Assessing the nonlinear response of fine particles to precursor emissions: development and application of an extended response surface modeling technique v1.0. *Geosci. Model Dev. (GMD)* 8 (1), 115–128. <https://doi.org/10.5194/gmd-8-115-2015>.
- Zhao, B., Wu, W.J., Wang, S.X., Xing, J., Chang, X., Liou, K.N., Jiang, J.H., Gu, Y., Jang, C., Fu, J.S., Zhu, Y., Wang, J.D., Lin, Y., Hao, J.M., 2017. A modeling study of the nonlinear response of fine particles to air pollutant emissions in the Beijing-Tianjin-Hebei region. *Atmos. Chem. Phys.* 17 (19), 12031–12050. <https://doi.org/10.5194/acp-17-12031-2017>.
- Zhao, B., Zheng, H.T., Wang, S.X., Smith, K.R., Lu, X., Aunan, K., Gu, Y., Wang, Y., Ding, D., Xing, J., Fu, X., Yang, X.D., Liou, K.N., Hao, J.M., 2018. Change in household fuels dominates the decrease in PM_{2.5} exposure and premature mortality in China in 2005–2015. *Proc. Natl. Acad. Sci. U.S.A.* 115 (49), 12401–12406. <https://doi.org/10.1073/pnas.1812955115>.
- Zhu, Y., Lao, Y.W., Jang, C., Lin, C.-J., Xing, J., Wang, S.X., Fu, J.S., Deng, S., Xie, J.P., Long, S.C., 2015. Development and case study of a science-based software platform to support policy making on air quality. *J. Environ. Sci. (China)* 27, 97–107. <https://doi.org/10.1016/j.jes.2014.08.016>.